# Impact of Pericoronary Adipose Tissue Attenuation on Periprocedural Myocardial Injury in Patients With Chronic Coronary Syndrome

Yamamoto, Tetsuya ; Kawamori, Hiroyuki ; Toba, Takayoshi ; Sasaki, Satoru ; Fujii, Hiroyuki ; Hamana, Tomoyo ; Osumi, Yuto ; Iwane, Seigo…

# Journal of the American Heart Association

## ORIGINAL RESEARCH

# Impact of Pericoronary Adipose Tissue Attenuation on Periprocedural Myocardial Injury in Patients With Chronic Coronary Syndrome

Tetsuya Yamamoto , MD; Hiroyuki Kawamori , MD, PhD; Takayoshi Toba , MD, PhD; Satoru Sasaki , MD; Hiroyuki Fujii , MD, PhD; Tomoyo Hamana , MD, PhD; Yuto Osumi , MD; Seigo Iwane , MD; Shota Naniwa , MD; Yuki Sakamoto , MD; Koshi Matsuhama , MD; Yuta Fukuishi, MD; Ken-ichi Hirata, MD, PhD; Hiromasa Otake , MD, PhD

**BACKGROUND:** Perivascular inflammation contributes to the development of atherosclerosis and microcirculatory dysfunction. Pericoronary adipose tissue (PCAT) attenuation, measured by coronary computed tomography angiography, is a potential indicator of coronary inflammation. However, the relationship between PCAT attenuation, microcirculatory dysfunction, and periprocedural myocardial injury (PMI) remains unclear.

**METHODS AND RESULTS:** Patients with chronic coronary syndrome who underwent coronary computed tomography angiography before percutaneous coronary intervention were retrospectively identified. PCAT attenuation and adverse plaque characteristics were assessed using coronary computed tomography angiography. The extent of microcirculatory dysfunction was evaluated using the angio-based index of microcirculatory resistance before and after percutaneous coronary intervention. Overall, 125 consecutive patients were included, with 50 experiencing PMI (PMI group) and 75 without PMI (non-PMI group). Multivariable analysis showed that older age, higher angio-based index of microcirculatory resistance, presence of adverse plaque characteristics, and higher lesion-based PCAT attenuation were independently associated with PMI occurrence (odds ratio [OR], 1.07 [95% CI, 1.01–1.13]; $P=0.02$; OR, 1.06 [95% CI, 1.00–1.12]; $P=0.04$; OR, 6.62 [95% CI, 2.13–20.6]; $P=0.001$; and OR, 2.89 [95% CI, 1.63–5.11]; $P<0.001$, respectively). High PCAT attenuation was correlated with microcirculatory dysfunction before and after percutaneous coronary intervention and its exacerbation during percutaneous coronary intervention. Adding lesion-based PCAT attenuation to the presence of adverse plaque characteristics improved the discriminatory and reclassification ability in predicting PMI.

**CONCLUSIONS:** Adding PCAT attenuation at the culprit lesion level to coronary computed tomography angiography-derived adverse plaque characteristics may provide incremental benefit in identifying patients at risk of PMI. Our results highlight the importance of microcirculatory dysfunction in PMI development, particularly in the presence of lesions with high PCAT attenuation.

**REGISTRATION:** URL: https://center6.umin.ac.jp/cgi-open-bin/ctr/ctr_view.cgi?recptno=R000057722; Unique identifier: UMIN000050662.

**Key Words:** adverse plaque characteristics ■ coronary computed tomography angiography ■ pericoronary adipose tissue ■ periprocedural myocardial injury

Percutaneous coronary intervention (PCI) effectively relieves symptoms and reduces the incidence of spontaneous myocardial infarction in patients with chronic coronary syndrome (CCS). However, periprocedural myocardial injury (PMI) occurs constantly, related to worse clinical outcomes

*JAHA* is available at: www.ahajournals.org/journal/jaha

## CLINICAL PERSPECTIVE

### What Is New?

- High baseline pericoronary adipose tissue attenuation is independently associated with periprocedural myocardial infarction.
- Microvascular dysfunction contributes to the development of periprocedural myocardial infarction, particularly in the context of lesions characterized by high pericoronary adipose tissue attenuation.

### What Are the Clinical Implications?

- Preoperative coronary computed tomography angiography evaluation, including pericoronary adipose tissue attenuation, has the potential to assist in determining the treatment strategy.
- It may be reasonable to defer invasive procedures in favor of statin treatment and plaque stabilization, or to guide optimal initiation of appropriate antiplatelet therapy, for chronic coronary syndrome patients with high pericoronary adipose tissue attenuation.

### Nonstandard Abbreviations and Acronyms

| | |
|---|---|
| **APC** | adverse plaque characteristic |
| **CCS** | chronic coronary syndrome |
| **IMR** | index of microcirculatory resistance |
| **PCAT** | pericoronary adipose tissue |
| **PMI** | periprocedural myocardial injury |
| **QFR** | quantitative flow ratio |

after PCI in these patients.[1] Previous studies have repeatedly reported that target plaque characteristics assessed using various imaging modalities can predict PMI after PCI. Nonetheless, adverse plaque characteristics (APCs) observed using these modalities at a single time point may not necessarily reflect the activity of the plaque during a long period of plaque development.[2] Therefore, accurate PMI prediction based solely on image-based plaque characterization remains challenging.[3–5]

The cause of PMI is currently considered multifactorial. Distal coronary embolization of atheromatous material and intracoronary thrombus can result in PMI through no-reflow/slow-flow phenomena during PCI. In addition, coronary vasospasm may be involved due to thrombosis, neuro-hormonal activation, and coronary microcirculatory dysfunction. Among several potential contributors, local inflammation is a key driver contributing to most of these underlying mechanisms.

Inflammation promotes plaque progression, increases plaque vulnerability and instability, and accelerates atheromatous embolization, thrombogenicity, and microcirculatory dysfunction.[6–8] Therefore, we hypothesized that assessing local vascular inflammation before PCI might enhance the predictive accuracy for PMI over the traditional plaque characterization-based approach using APCs.

Recent advancements in coronary computed tomography angiography (cCTA) have allowed for noninvasive evaluation of the local inflammatory status of coronary arteries. Notably, several previous studies have shown that cCTA has the feasibility of measuring epicardial adipose tissue that closely overlays coronary arteries, known as pericoronary adipose tissue (PCAT). PCAT is closely opposed to the coronary arteries; therefore, PCAT attenuation on cCTA indicates inflammatory activity within the underlying vascular wall. Previous studies reported a significant association between increased PCAT attenuation and future adverse events in patients with coronary artery disease.[9,10] Therefore, we aimed to clarify the relationship between PCAT attenuation before PCI and the occurrence of PMI. In addition, we evaluated the extent of microcirculatory dysfunction before and after PCI using a single-view Murray's law-based quantitative flow ratio (µQFR) analysis. The objective was to elucidate the interplay between APC, local inflammation, and microcirculatory dysfunction in developing PMI.

## METHODS

### Study Design

This retrospective, single-center, observational study included consecutive patients with CCS who underwent cCTA before PCI. The study period was between January 2014 and December 2020. The inclusion criteria were patients with CCS who (1) underwent PCI with a drug-eluting stent, (2) underwent cCTA within 90 days before PCI, (3) underwent serial measurements of high-sensitivity cardiac troponin I (cTnI) before PCI and within 48 hours after PCI, and (4) were aged ≥20 years. The exclusion criteria are described in Data S1. The cTnI measurements were not explicitly ordered based on symptoms, ECG changes, or other specific indications. However, they were routinely obtained as part of our institution's standard protocol for PCI procedures. This study protocol complied with the Declaration of Helsinki and was approved by the Ethics Committee of Kobe University Hospital. Informed consent was obtained in the form of an opt-out on the website of the Division of Cardiovascular Medicine, Kobe University Graduate School of Medicine. This study was registered in the University Hospital Medical Information Network Clinical Trial Registry (UMIN000050662). The data that support

the findings of this study are available from the corresponding author on reasonable request.

## Angiogram Analysis

In this study, µQFR analysis was performed using the QFR software (AngioPlus Core, version V3; Shanghai Pulse Medical Technology, Shanghai, China). The research was conducted by 2 experienced and certified analysts blinded to patients' clinical characteristics pre- and post-PCI. The detailed methodology for single-view µQFR computation has been previously described.[11–13]

Angiographic microvascular resistance was computed as $P_d$ divided by the hyperemic flow velocity (Velocity$_{hyp}$).

$$\text{Angiographic microvascular resistance (mm Hg×s/cm)}$$
$$= P_d/\text{Velocity}_{hyp} = P_a \times \mu QFR/\text{Velocity}_{hyp}.$$

The index of microcirculatory resistance (IMR) can be calculated as IMR [mm Hg×s/cm]=[angiographic microvascular resistance−0.9]/0.07, as previously reported.[14] In this computation, an average aorta pressure of 86 mm Hg during maximum hyperemia is assumed.[15] Δ IMR value was calculated as post-PCI IMR minus pre-PCI IMR.

In addition to the µQFR analysis, quantitative coronary angiography data were also available from the software. Quantitative coronary angiography included reference vessel diameter, minimum lumen diameter, percent diameter stenosis, and acute gain. The acute gain was defined as the difference between the minimum lumen diameter pre- and post-PCI. Transient no-reflow was described as an angiogram showing a deterioration of coronary flow of Thrombolysis In Myocardial Infarction (TIMI) grade 0, 1, or 2 during the procedure, regardless of the timing, and TIMI grade 3 at the final angiogram. The final slow flow was defined as an angiogram showing a deterioration of coronary flow of TIMI grade 1 or 2 at the final angiogram.[5]

## cCTA Imaging Acquisition

Initially, a noncontrast cardiac computed tomography (CT) was performed to assess the extent of coronary calcification through the Agatston coronary calcium score. cCTA images were obtained following the Society of Cardiovascular Computed Tomography guidelines on cCTA.[16] Oral β-blockers were administered in subjects with heart rates ≥65 beats per minute. Immediately before cCTA acquisition, 0.3 mg sublingual nitroglycerine was administered to all patients. cCTA was performed using retrospective ECG-gated spiral acquisition. All examinations were performed with Somatom Definition Flash (128×0.6 mm section collimation; Siemens, Forchheim, Germany). The scan parameters included 70 to 120 kilovolt peak (kVp) tube voltage and 260 to 1150 mA tube current (depending on body habitus). All images were reconstructed using thin slices (0.5–0.75 mm) and medium smooth reconstruction filters in different phases.

## cCTA Image Analysis of Plaque Characteristics

The cCTA image analysis was performed using a semiautomated plaque analysis workstation (SYNAPSE VINCENT; Fujifilm, Tokyo, Japan) with an additional minor manual optimization to obtain qualitative plaque features. cCTA images were analyzed by 2 independent investigators blinded to patients' clinical characteristics except for the information on the culprit lesion location. The plaque measurements included absolute volumes (in cubic millimeters) and the corresponding burden (plaque volume×100%/vessel volume) of calcified plaques (>350 Hounsfield units [HU]) and noncalcified plaques (≤350 HU), as well as the remodeling index, lesion length, and diameter stenosis. Noncalcified plaques were further divided into their components: low-attenuation plaque (−30 to 30 HU), intermediate-attenuation plaque (31–130 HU), and high-attenuation plaque (131–350 HU) volumes, and the corresponding plaque burden.[17] The presence of APCs (low-attenuation plaque, positive remodeling, spotty calcification, and napkin-ring sign) was assessed in each lesion following the definitions from previous studies.[2,18] A detailed methodology of cCTA image analysis is described in the Supplemental Material.

## PCAT Analysis

PCAT analysis was performed using a workstation (SYNAPSE VINCENT; Fujifilm, Tokyo, Japan). To measure PCAT attenuation, 3-dimensional layers within radial distance from the outer coronary wall equal in thickness to the average diameter of the vessel were constructed automatically from the CTA. Within the predefined volume of interest, voxels with tissue attenuation ranging from −190 to −30 HU were considered adipose tissue. The automated analysis did not include the myocardial tissue adjacent to the vessel wall and the coronary branches originating from the vessel of interest. PCAT attenuation was defined as the mean attenuation within such contamination-free volumes of interest. These measurements were performed in each patient around the specific culprit lesions (PCAT$_{Lesion}$), the proximal culprit vessels (PCAT$_{Vessel}$), and the proximal right coronary artery (RCA) (PCAT$_{RCA}$). PCAT$_{Vessel}$ and PCAT$_{RCA}$ were measured to compare the diagnostic ability for the occurrence of PMI among lesion, vessel, and patient-level PCAT attenuation. PCAT$_{Lesion}$ was measured around target lesions, with the proximal

and distal borders of the analysis region defined as the proximal and distal ends of the lesion.[19,20] The proximal 40-mm segments of the left anterior descending coronary artery and left circumflex coronary artery, and the proximal 10- to 50-mm segment of the RCA were traced, as previously described.[9] $PCAT_{RCA}$ represented PCAT measurements at the patient level.[9,10] Inter- and intraobserver variabilities in assessing PCAT attenuation for all cases were quantified using κ concordance analysis.

## Outcomes

The study's primary outcome was the occurrence of PMI. PMI was defined as >5×99th percentile upper reference limit increase of high-sensitivity cTnI values within 48 hours after PCI in patients with CCS with normal baseline cTnI values[1] (normal reference range: <24 pg/mL).

## Statistical Analysis

All statistical analyses were performed using the Microsoft R open software version 3.4.1 (R Development Core Team, Vienna, Austria). Continuous variables are presented as mean±SD or median (25th, 75th percentiles) and compared using the Student $t$ test for normally distributed data or the Mann-Whitney $U$ test for nonnormally distributed data. Data at different time points were analyzed using the paired Student $t$ test or Wilcoxon test, as appropriate. Categorical variables are presented as frequencies with percentages and were compared using the $\chi^2$ or Fisher exact test, as appropriate. Statistical significance was set at a 2-sided $P$ value <0.05. The variables included in the multivariable logistic regression analysis encompassed baseline clinical characteristics (age, hypertension, dyslipidemia, diabetes, current smoking), cCTA findings (lesion length, percent diameter stenosis, total plaque volume, low-attenuation plaque volume, presence of any APCs), PCAT variables, and pre-PCI IMR. Within the multivariable logistic regression analysis, significant correlations emerged among specific covariates. The presence of any APCs, which encompasses individual components of APCs such as low-attenuation plaque, positive remodeling, spotty calcification, and the napkin-ring sign, were identified as related factors. Additionally, significant correlations were observed among $PCAT_{Lesion}$, $PCAT_{Vessel}$, and $PCAT_{RCA}$. To comprehensively investigate the relationship between each variable and the occurrence of PMI, we used multiple models, which are as follows: Model A (comprising low-attenuation plaque, positive remodeling, spotty calcification, napkin-ring sign, and $PCAT_{Lesion}$), Model B (involving the presence of any APCs and $PCAT_{Lesion}$), Model C (involving the presence of any APCs and $PCAT_{Vessel}$), and Model D (involving the presence of any

APCs and $PCAT_{RCA}$). The area under the curve (AUC) was calculated from receiver operating characteristic (ROC) curve analysis for $PCAT_{Lesion}$, $PCAT_{Vessel}$, and $PCAT_{RCA}$, and compared using the DeLong method. Three prediction models for PMI were constructed to determine the incremental discriminatory and reclassification performance of PCAT attenuation. As a baseline, clinical Model 1 was derived from cardiovascular risk factors (age, hypertension, diabetes, dyslipidemia, and current smoking) and quantitative cCTA analysis (lesion length, percent diameter stenosis, and total plaque volume). Clinical Model 2 was constructed using clinical Model 1 + cCTA plaque quality analysis (the presence of APCs and low-attenuation plaque volume). Clinical Model 3 was derived from clinical Model 2 + PCAT attenuation at the culprit lesion level. The discriminatory ability of Models 2 and 3 was assessed by ROC analysis, and the reclassification performance of each model was compared using the relative integrated discrimination improvement and category-free net reclassification index. ROC analysis was used to determine the optimal cutoff value of $PCAT_{Lesion}$ associated with PMI according to tube voltage as follows: 70 or 100 to 120 kVp.

## RESULTS

### Study Population

In total, 253 patients with CCS underwent PCI with prior cCTA within 90 days before PCI during the study period. Among them, 201 patients had serial cTnI measurements performed before PCI and within 48 hours after PCI and met the inclusion criteria. After excluding patients based on various criteria, including patients with a positive cTnI before PCI (n=9), patients with coronary artery bypass graft lesions (n=7), patients with chronic total occlusion (n=11), patients with in-stent restenosis (n=3), patients with severely calcified lesions (n=16), patients with left main trunk lesions (n=10), patients with >1 main coronary artery intervention during single PCI procedure (n=9), patients with side branch occlusion during PCI procedure (n=3), patients with cardiogenic shock during PCI (n=2), and patients with insufficient CT data quality (n=6), 125 patients were finally included in the analysis. Among these patients, 50 (40.0%) experienced PMI (PMI group), whereas 75 (60.0%) did not experience PMI (non-PMI group) (Figure S1).

### Comparison of Baseline Characteristics Between PMI and Non-PMI Groups

The baseline patient characteristics are shown in Table 1. Patients with PMI were significantly older than those with non-PMI. The prevalence of coronary risk factors and medications on admission were similar

between the 2 groups. CK-MB and cTnI levels before PCI were comparable between the 2 groups; however, those after PCI in the PMI group were significantly higher than those in the non-PMI group (7.5 [5–11] U/L versus 4 [4–4.5] U/L, *P*<0.001; 920 [482.5–1890] ng/mL versus 70 [45–80] ng/mL, *P*<0.001; respectively).

The baseline lesion, procedural, and angiographic characteristics are shown in Table 2. The 2 groups had no significant differences in target vessels, lesion location, number of implanted stents, and stent diameter. Stent length in the PMI group was significantly longer than that in the non-PMI group. The occurrence of transient no-reflow and final slow flow was significantly higher in the PMI group than in the non-PMI group. Pre-PCI reference vessel diameter, minimum lumen diameter, percent diameter stenosis, and µQFR were comparable; however, pre-PCI IMR was significantly

higher in the PMI group than in the non-PMI group. In addition, post-PCI IMR and Δ IMR were significantly higher in the PMI group than in the non-PMI group. IMR levels were significantly increased during PCI in the PMI group but not in the non-PMI group (Table 2). If patients with transient or final no-reflow phenomenon were excluded, post-PCI IMR values remained higher in the PMI group (n=39) than those in the non-PMI group (n=74) (42.9±10.4 mm Hg×s/cm versus 27.0±6.7 mm Hg×s/cm, *P*<0.001).

## Comparison of cCTA Findings Between PMI and Non-PMI Groups

Table 3 summarizes cCTA findings. The 2 groups had no statistically significant differences in percent diameter stenosis, lesion external elastic membrane

**Table 1.  Baseline Patient Characteristics**

| Variables | All lesions (n=125) | PMI (n=50) | Non-PMI (n=75) | *P* value |
|---|---|---|---|---|
| Baseline patient characteristics | | | | |
| Age, y | 69.0±9.2 | 73.0±8.6 | 69.1±11.4 | 0.046 |
| Sex, male, n (%) | 95 (76.0%) | 36 (72.0%) | 59 (78.7%) | 0.40 |
| Hypertension, n (%) | 89 (71.2%) | 36 (72.0%) | 53 (70.1%) | 0.87 |
| Dyslipidemia, n (%) | 87 (69.6%) | 36 (72.0%) | 51 (68.0%) | 0.64 |
| Diabetes, n (%) | 54 (43.2%) | 22 (44.0%) | 32 (42.3%) | 0.88 |
| Current smoker, n (%) | 58 (46.4%) | 24 (48.0%) | 34 (45.3%) | 0.77 |
| Prior PCI, n (%) | 20 (16.0%) | 11 (22.0%) | 9 (12.0%) | 0.14 |
| Chronic kidney disease, n (%) | 48 (38.4%) | 20 (40.0%) | 28 (37.3%) | 0.77 |
| Hemodialysis, n (%) | 6 (4.8%) | 4 (8.0%) | 2 (2.7%) | 0.18 |
| LVEF, % | 59.7±8.7 | 58.4±10.8 | 60.5±6.9 | 0.18 |
| Laboratory data | | | | |
| BNP, pg/mL | 40.5 (18.8, 96.1) | 43.4 (21.4, 136.9) | 36.1 (18.8, 88.9) | 0.23 |
| Estimated GFR, mL/min per 1.73 m² | 60.6±18.2 | 59.9±21.1 | 61.2±15.9 | 0.70 |
| Low-density lipoprotein cholesterol, mg/dL | 105.8±30.3 | 104.9±29.5 | 106.4±30.8 | 0.78 |
| High-density lipoprotein cholesterol, mg/dL | 46.6±12.7 | 46.5±11.9 | 46.7±13.1 | 0.94 |
| HbA1c, % | 6.4±1.1 | 6.3±1.0 | 6.5±1.2 | 0.32 |
| WBC count, per µL | 6212±1764 | 6281±1667 | 6110±1895 | 0.60 |
| hs-CRP, mg/L | 0.50±1.56 | 0.52±1.46 | 0.49±1.63 | 0.91 |
| Pre-CK-MB, U/L | 4 (4, 5) | 4 (4, 5) | 4 (4, 5) | 0.68 |
| Pre-cTnI, pg/mL | 10 (10, 20) | 10 (10, 20) | 10 (10, 20) | 0.71 |
| Post-CK-MB, U/L | 4 (4, 7) | 7.5 (5, 11) | 4 (4, 4.5) | <0.001 |
| Post-cTnI, pg/mL | 90 (60, 700) | 920 (482.5, 1890) | 70 (45, 80) | <0.001 |
| Medications | | | | |
| Statins, n (%) | 72 (57.6%) | 29 (58.0%) | 43 (57.3%) | 0.94 |
| β-Blockers, n (%) | 67 (53.6%) | 27 (54.0%) | 40 (53.3%) | 0.94 |
| RAS inhibitors, n (%) | 72 (57.6%) | 26 (52.0%) | 46 (61.3%) | 0.30 |
| Calcium channel blockers, n (%) | 54 (43.2%) | 22 (44.0%) | 32 (42.7%) | 0.88 |

Values are expressed as mean±SD, median (25th, 75th percentiles), or n (%). BNP indicates brain-type natriuretic peptide; CK-MB, creatine kinase-MB; cTnI, cardiac troponin I; GFR, glomerular filtration rate; HbA1c, hemoglobin A1c; LVEF, left ventricular ejection fraction; hs-CRP, high-sensitivity C-reactive protein; PCI, percutaneous coronary intervention; PMI, periprocedural myocardial injury; RAS, renin-angiotensin system; and WBC, white blood cell.

**Table 2.   Lesion, Procedural, and Angiographic Characteristics**

| Variables | All lesions (n=125) | PMI (n=50) | Non-PMI (n=75) | *P* value |
|---|---|---|---|---|
| Lesion characteristics | | | | |
| Target vessel: LAD/LCX/RCA, % | 53.6/16.0/30.4 | 56.0/20.0/24.0 | 52.0/13.3/34.7 | 0.39 |
| Lesion location: proximal/mid/distal, % | 36.8/56.8/6.4 | 30.0/66.0/4.0 | 41.3/50.7/8.0 | 0.24 |
| Multivessel disease | 73 (58.4%) | 30 (60%) | 43 (57.3%) | 0.77 |
| Procedural characteristics | | | | |
| No. of stents | 1.21±0.43 | 1.28±0.45 | 1.16±0.40 | 0.12 |
| Stent diameter, mm | 3.10±0.43 | 3.03±0.35 | 3.15±0.48 | 0.14 |
| Stent length, mm | 30.0±14.5 | 34.2±14.9 | 27.1±13.5 | 0.007 |
| Distal protection device, n (%) | 13 (10.4%) | 7 (14.0%) | 6 (8.0%) | 0.29 |
| Angiographic analysis | | | | |
| Pre-PCI | | | | |
| Reference vessel diameter, mm | 2.68±0.49 | 2.58±0.44 | 2.75±0.51 | 0.17 |
| Minimum lumen diameter, mm | 1.08±0.40 | 0.98±0.31 | 1.04±0.25 | 0.20 |
| Diameter stenosis, % | 57.6±11.9 | 59.3±10.0 | 57.2±11.1 | 0.30 |
| Post-PCI | | | | |
| Minimum lumen diameter, mm | 2.39±0.39 | 2.34±0.27 | 2.42±0.45 | 0.29 |
| Diameter stenosis, % | 14.6±11.1 | 15.3±10.9 | 14.1±11.2 | 0.57 |
| Transient no-reflow, n (%) | 12 (9.6%) | 11 (22.0%) | 1 (1.3%) | <0.01 |
| Final slow flow, n (%) | 5 (4.0%) | 5 (10.0%) | 0 (0.0%) | 0.005 |
| Acute gain, mm | 1.36±0.58 | 1.43±0.48 | 1.31±0.63 | 0.27 |
| QFR analysis | | | | |
| µQFR pre-PCI | 0.68±0.16 | 0.69±0.13 | 0.68±0.17 | 0.96 |
| µQFR post-PCI | 0.89±0.09 | 0.92±0.06 | 0.87±0.10 | 0.01 |
| IMR analysis | | | | |
| IMR pre PCI, mm Hg×s/cm | 29.8±9.7 | 34.5±8.1 | 26.6±9.5 | <0.001 |
| IMR post-PCI, mm Hg×s/cm | 33.4±11.5 | 43.0±10.5* | 27.0±6.6 | <0.001 |
| ΔIMR, mm Hg×s/cm | 3.6±9.3 | 8.6±9.4 | 0.4±7.6 | <0.001 |

Values are expressed as mean±SD or n (%). µQFR indicates Murray's law-based quantitative flow ratio; IMR, index of microvascular resistance; LAD, left anterior descending artery; LCX, left circumflex artery; PCI, percutaneous coronary intervention; PMI, periprocedural myocardial injury; QFR, quantitative flow ratio; and RCA, right coronary artery.

*Indicates *P*<0.05 vs IMR pre-PCI.

CSA, minimum lumen area, and total plaque volume. However, lesion length and remodeling index were significantly greater, low-attenuation plaque volume was numerically larger, and the CT attenuation value of the culprit plaque was significantly lower in the PMI group than in the non-PMI group. Spotty calcification and plaques with napkin-ring signs were significantly more frequent in the PMI group than in the non-PMI group. In addition, the prevalence of any APCs was significantly higher in the PMI group than in the non-PMI group (72.0% versus 50.7%, *P*=0.017). As for PCAT attenuation, PCAT$_{Lesion}$, PCAT$_{Vessel}$, and PCAT$_{RCA}$ were significantly higher in the PMI group than in the non-PMI group (all *P* values <0.01). Inter- and intraobserver agreements for measuring PCAT attenuation were within the acceptable range (PCAT$_{Lesion}$: intraobserver, 0.975; interobserver, 0.918; PCAT$_{Vessel}$: intraobserver, 0.980;

interobserver, 0.930; PCAT$_{RCA}$: intraobserver, 0.988; interobserver, 0.955).

## Factors Associated With PMI

The results of the univariate and multivariable logistic regression analysis examining clinical factors and cCTA findings associated with PMI are summarized in Table 4. The multivariable Model A showed that age, pre-PCI IMR, and PCAT$_{Lesion}$ were independently associated with PMI. The multivariable Models B, C, and D showed that in addition to older age, the presence of any APCs, pre-PCI IMR, and PCAT-related variables such as PCAT$_{Lesion}$ (Model B; odds ratio [OR], 2.89 [95% CI, 1.63–5.11]; *P*<0.001), PCAT$_{Vessel}$ (Model C; OR, 1.96 [95% CI, 1.22–3.16]; *P*=0.006), and PCAT$_{RCA}$ (Model D; OR, 1.69 [95% CI, 1.14–2.53]; *P*=0.010) were independently associated with the occurrence of PMI. To improve the validity

**Table 3.  cCTA Findings**

| Variables | All lesions (n=125) | PMI (n=50) | Non-PMI (n=75) | P value |
|---|---|---|---|---|
| cCTA settings | | | | |
| Tube voltage, n (%) | | | | 0.46 |
| 70 kVp | 61 (48.8%) | 21 (42%) | 40 (53.3%) | |
| 100–120 kVp | 64 (51.2%) | 29 (58%) | 35 (46.7%) | |
| Quantitative cCTA analysis | | | | |
| Lesion length, mm | 24.6±11.0 | 27.6±11.9 | 22.6±9.8 | 0.012 |
| Diameter stenosis, % | 72.0±19.0 | 72.6±21.2 | 71.5±17.4 | 0.77 |
| Lesion EEM CSA, m$^2$ | 11.5±5.2 | 11.8±5.1 | 11.3±5.2 | 0.65 |
| Lesion MLA, m$^2$ | 1.05±0.72 | 0.94±0.49 | 1.12±0.83 | 0.18 |
| Remodeling index | 1.13±0.35 | 1.20±0.35 | 1.08±0.34 | 0.048 |
| CT attenuation value, HU | 58.1±29.1 | 44.4±26.2 | 67.2±27.3 | <0.001 |
| Coronary artery calcium score | 341 (51, 808) | 341 (61, 707) | 327 (48, 954) | 0.82 |
| Total plaque volume, mm$^3$ | 261.9±144.9 | 272.1±140.3 | 255.0±147.6 | 0.52 |
| cCTA plaque quality analysis | | | | |
| Plaque composition volume, mm$^3$ | | | | |
| Low-attenuation plaque | 53.9±16.0 | 57.3.±15.3 | 51.6±16.1 | 0.052 |
| Intermediate-attenuation plaque | 80.2±72.1 | 83.2±59.2 | 78.2±79.3 | 0.71 |
| High-attenuation plaque | 109.1±84.9 | 113.5±83.1 | 106.2±86.0 | 0.64 |
| Calcified plaque | 18.7±28.5 | 18.2±26.7 | 19.1±29.6 | 0.87 |
| Plaque composition burden, % | | | | |
| Low-attenuation plaque | 26.4±17.2 | 27.6±21.2 | 25.6±13.8 | 0.52 |
| Intermediate-attenuation plaque | 28.9±17.1 | 29.9±17.4 | 28.3±16.9 | 0.60 |
| High-attenuation plaque | 37.9±13.7 | 36.5±15.8 | 39.0±12.0 | 0.32 |
| Calcified plaque | 6.7±9.5 | 6.0±8.0 | 7.2±10.3 | 0.49 |
| Presence of APCs | 74 (59.2%) | 36 (72.0%) | 38 (50.7%) | 0.017 |
| Positive remodeling, n (%) | 49 (39.2%) | 24 (48.0%) | 25 (33.3%) | 0.10 |
| Low attenuation plaque, n (%) | 27 (21.6%) | 15 (30.0%) | 12 (16.0%) | 0.063 |
| Spotty calcification, n (%) | 41 (32.8%) | 24 (52.2%) | 17 (22.7%) | 0.011 |
| Napkin-ring sign, n (%) | 20 (16.0%) | 12 (24.0%) | 8 (10.7%) | 0.047 |
| PCAT attenuation analysis | | | | |
| PCAT$_{Lesion}$, HU | −81.3±11.4 | −75.9±10.9 | −84.9±10.3 | <0.001 |
| PCAT$_{Vessel}$, HU | −82.8±11.7 | −79.1±11.7 | −85.3±11.1 | 0.004 |
| 2003PCAT$_{RCA}$, HU | −83.1±11.1 | −78.9±10.1 | −85.7±11.0 | <0.001 |

Values are expressed as mean±SD, median (25th, 75th percentiles), or n (%). APCs indicates adverse plaque characteristics; cCTA, coronary computed tomography angiography; CSA, cross sectional area; EEM, external elastic membrane; HU, Hounsfield units; kVp, kilovolt peak; MLA, minimum lumen area; PCAT, pericardial adipose tissue; PMI, periprocedural myocardial injury; and RCA, right coronary artery.

and interpretability of the results, we have reduced the variables in the multivariable models in Table S1. After reducing the variables, the multivariable model consistently showed that PCAT$_{Lesion}$ (OR, 2.50 [95% CI, 1.48–4.21]; $P<0.001$) was independently associated with the occurrence of PMI (Table S1). The AUC of the presence of any APCs for identifying PMI was 0.61 (95% CI, 0.52–0.69), and the sensitivity, specificity, positive predictive value, and negative predictive value of the presence of any APCs alone were 72.0%, 49.3%, 48.6%, and 72.5%, respectively. The AUC of PCAT$_{Lesion}$ for identifying PMI was significantly

higher than that of PCAT$_{Vessel}$ and PCAT$_{RCA}$ in diagnostic performance (Figure 1).

## Discriminatory Diagnostic Ability by the Addition of Factors for PMI

Three prediction models were constructed to determine the incremental discriminatory and reclassification performance of cCTA findings and PCAT attenuation. Figure 2 shows ROC curves for the 3 models and their predictive performance. Compared with Model 1 (cardiovascular risk factors and quantitative cCTA analysis),

**Table 4. Uni- and Multivariable Logistic Regression Analysis of Baseline Patient Characteristics, cCTA Findings, and Angiogram Analysis Associated With PMI**

| Variables | Univariate analysis OR (95% CI) | P value | Multivariable Model A OR (95% CI) | P value | Multivariable Model B OR (95% CI) | P value | Multivariable Model C OR (95% CI) | P value | Multivariable Model D OR (95% CI) | P value |
|---|---|---|---|---|---|---|---|---|---|---|
| Baseline patient characteristics | | | | | | | | | | |
| Age | 1.04 (1.00–1.08) | 0.049 | 1.09 (1.02–1.16) | 0.01 | 1.07 (1.01–1.13) | 0.02 | 1.05 (1.00–1.11) | 0.04 | 1.04 (0.99–1.09) | 0.12 |
| Hypertension | 1.07 (0.48–2.36) | 0.87 | 0.95 (0.23–3.11) | 0.93 | 1.03 (0.33–3.18) | 0.96 | 0.97 (0.33–2.82) | 0.96 | 1.02 (0.35–2.97) | 0.97 |
| Dyslipidemia | 1.21 (0.55–2.65) | 0.63 | 1.00 (0.28–3.52) | 1.00 | 1.33 (0.45–3.91) | 0.60 | 1.29 (0.46–3.66) | 0.63 | 1.33 (0.46–3.86) | 0.59 |
| Diabetes | 1.06 (0.51–2.17) | 0.88 | 1.11 (0.38–3.25) | 0.85 | 1.37 (0.50–3.74) | 0.54 | 1.50 (0.56–4.02) | 0.42 | 1.49 (0.55–4.02) | 0.43 |
| Current smoking | 1.11 (0.54–2.28) | 0.77 | 1.10 (0.36–3.39) | 0.87 | 0.85 (0.32–2.30) | 0.75 | 0.92 (0.36–2.33) | 0.86 | 1.00 (0.39–2.57) | 0.99 |
| cCTA findings | | | | | | | | | | |
| Lesion length (per 5-mm increase) | 1.24 (1.01–1.46) | 0.015 | 1.69 (0.87–2.43) | 0.07 | 1.36 (0.99–1.85) | 0.06 | 1.32 (0.99–1.76) | 0.06 | 1.35 (0.99–1.80) | 0.06 |
| Diameter stenosis, % (per 1% increase) | 1.00 (0.98–1.02) | 0.76 | 0.99 (0.96–1.02) | 0.46 | 0.99 (0.97–1.02) | 0.56 | 0.99 (0.97–1.02) | 0.54 | 0.99 (0.96–1.02) | 0.42 |
| Total plaque volume (per 1-m³ increase) | 1.00 (0.99–1.00) | 0.52 | 0.99 (0.99–1.02) | 0.12 | 0.99 (0.99–1.00) | 0.15 | 1.00 (0.99–1.00) | 0.18 | 1.00 (0.99–1.00) | 0.31 |
| Low-attenuation plaque volume (per 1-m³ increase) | 1.02 (0.99–1.05) | 0.06 | 1.02 (0.98–1.05) | 0.34 | 1.01 (0.98–1.04) | 0.48 | 1.02 (0.99–1.05) | 0.29 | 1.02 (0.99–1.05) | 0.24 |
| Presence of any APCs | 2.50 (1.16–5.38) | 0.019 | | | 6.62 (2.13–20.6) | 0.001 | 5.49 (1.90–15.9) | 0.002 | 5.69 (1.96–16.5) | 0.001 |
| Low-attenuation plaque | 2.25 (0.95–5.34) | 0.066 | 3.71 (0.99–13.8) | 0.06 | | | | | | |
| Positive remodeling | 1.85 (0.89–3.85) | 0.10 | 3.65 (0.90–12.8) | 0.07 | | | | | | |
| Spotty calcification | 2.68 (1.23–5.83) | 0.013 | 1.63 (0.49–5.47) | 0.43 | | | | | | |
| Napkin-ring sign | 2.64 (0.99–7.04) | 0.052 | 5.37 (0.98–26.9) | 0.06 | | | | | | |
| PCAT analysis | | | | | | | | | | |
| PCAT$_{Lesion}$ (per 10-HU increase) | 2.30 (1.53–3.45) | <0.001 | 2.98 (1.64–5.42) | <0.001 | 2.89 (1.63–5.11) | <0.001 | | | | |
| PCAT$_{Vessel}$ (per 10-HU increase) | 1.63 (1.16–2.29) | 0.005 | | | | | 1.96 (1.22–3.16) | 0.006 | | |
| PCAT$_{RCA}$ (per 10-HU increase) | 1.49 (1.11–2.0) | 0.008 | | | | | | | 1.69 (1.14–2.53) | 0.010 |
| Pre-PCI IMR (per 5-mmHg×s/cm increase) | 1.61 (1.28–2.02) | <0.001 | 1.06 (1.02–1.12) | 0.03 | 1.06 (1.00–1.12) | 0.04 | 1.08 (1.02–1.14) | 0.005 | 1.09 (1.03–1.15) | 0.003 |

APC indicates adverse plaque characteristics; cCTA, coronary computed tomography angiography; HU, Hounsfield units; IMR, index of microcirculatory resistance; OR, odds ratio; PCAT, pericoronary adipose tissue; PCI, percutaneous coronary intervention; PMI, periprocedural myocardial injury; and RCA, right coronary artery.
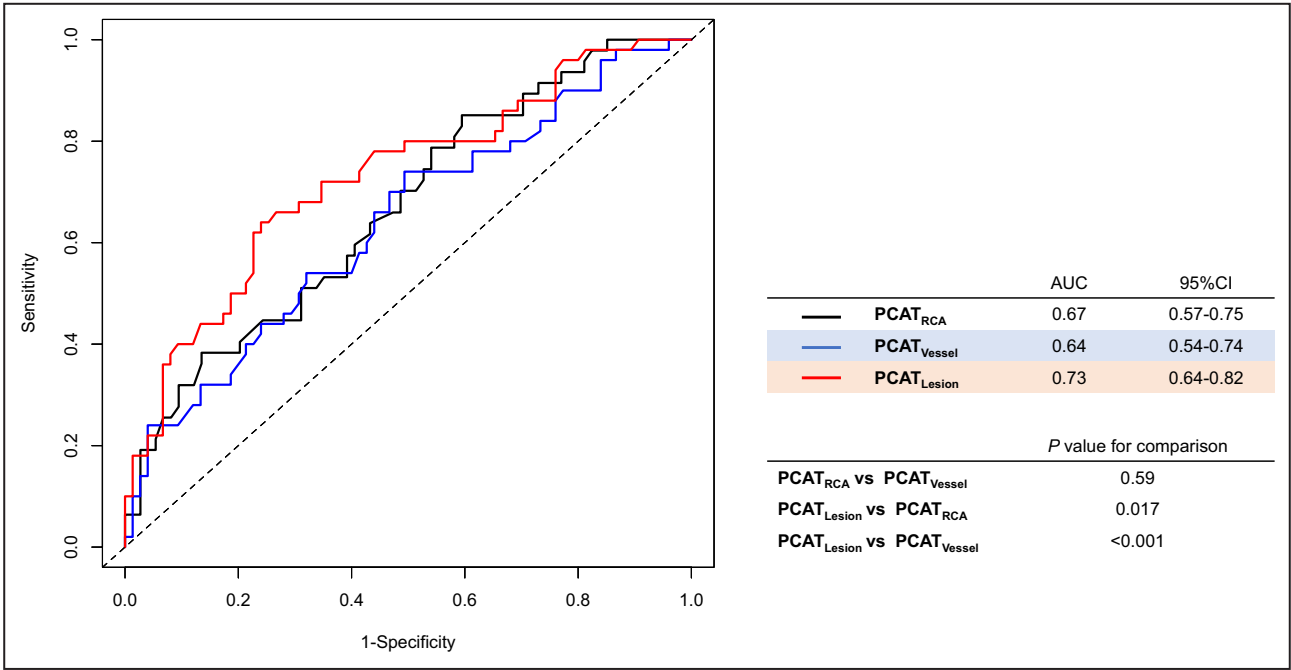
**Figure 1.  Diagnostic ability of PCAT attenuation at the culprit lesion, culprit vessel, and patient levels to identify PMI.**
Comparison of PCAT$_{Lesion}$, PCAT$_{Vessel}$, and PCAT$_{RCA}$ receiver operating characteristic curves and the AUCs are shown. AUC indicates area under the curve; PCAT, pericoronary adipose tissue; PMI, periprocedural myocardial injury; and RCA, right coronary artery.

Model 2 (Model 1+ cCTA plaque quality analysis) showed a numerically higher discriminatory ability (AUC: 0.74 versus 0.67; $P$=0.06) and a significantly higher reclassification ability (net reclassification index: 0.49; $P$=0.005; relative integrated discrimination improvement: 0.08; $P$<0.001) for identifying the occurrence of PMI. In addition, Model 3 (Model 2 + PCAT$_{Lesion}$) showed a significant increase in discriminatory ability
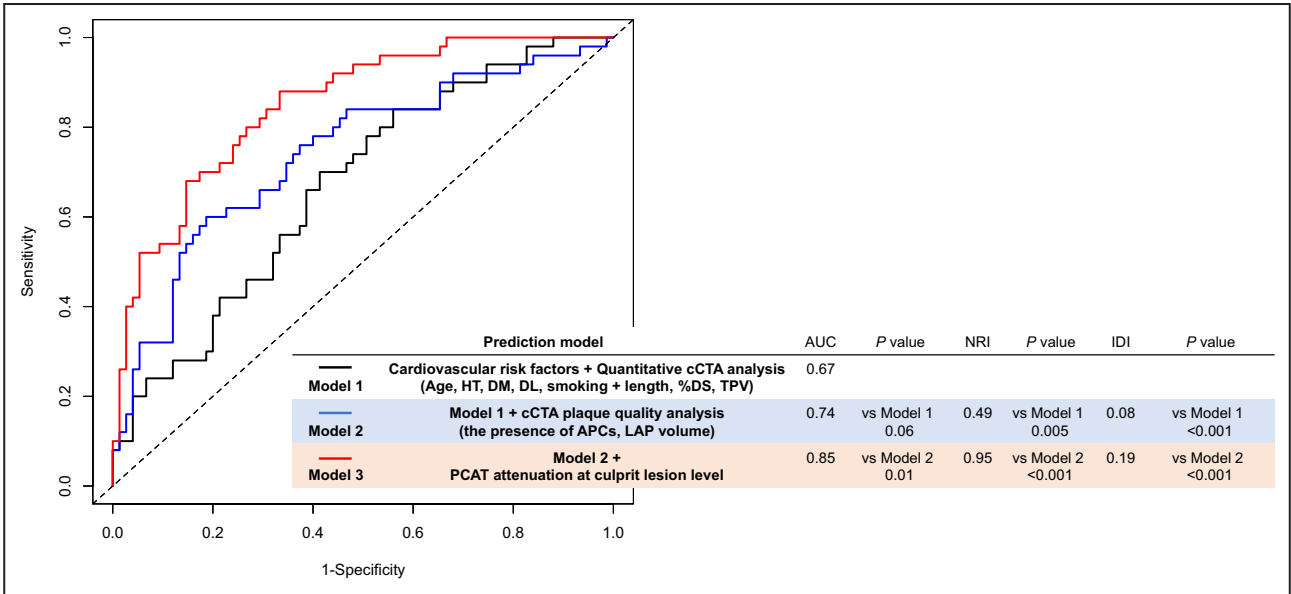


**Figure 2.  Comparison between discriminant and reclassification ability of predictive models for the presence of PMI.**
To determine incremental discriminatory and reclassification capacities of PCAT attenuation at the culprit lesion level, we constructed 3 analytical models as follows: Model 1: cardiovascular risk factors and quantitative cCTA analysis (black line); Model 2: Model 1 + cCTA plaque quality analysis (blue line); Model 3: Model 2+PCAT attenuation at culprit lesion level (red line). %DS indicates percent diameter stenosis; APCs, adverse plaque characteristics; AUC, area under the curve; cCTA, coronary computed tomography angiography; DL, dyslipidemia; DM, diabetes mellitus; HT, hypertension; IDI, integrated discrimination improvement; LAP, low-attenuation plaque; NRI, net reclassification index; PCAT, pericoronary adipose tissue; PMI, periprocedural myocardial injury; and TPV, total plaque volume.
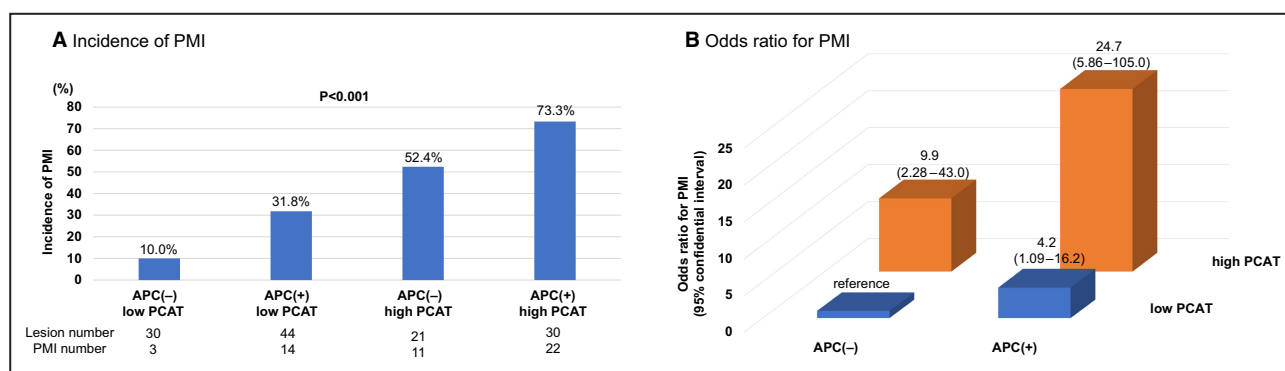
**Figure 3.  Incidence of PMI and the risk for PMI according to the presence of APCs and PCAT attenuation grade.**
**A**, Incidence of PMI. All lesions were classified according to the presence of APCs and PCAT attenuation grade. The incidence of PMI was significantly higher in lesions with APCs and high PCAT. **B**, Odds ratio for PMI. Lesions with APCs and high PCAT attenuation showed significantly higher risk than those with no APCs and low PCAT. APC indicates adverse plaque characteristic; PCAT, pericoronary adipose tissue; and PMI, periprocedural myocardial injury.

(AUC: 0.85 versus 0.74; $P=0.01$) and incremental re-classification ability (net reclassification index: 0.95; $P<0.001$; relative integrated discrimination improvement: 0.19; $P<0.001$) compared with Model 2 (Figure 2). When limiting the predictive model to the most important variables, PCAT continued to demonstrate incremental predictive value (Figure S2).

## Incidence of PMI and the Risk for PMI According to the Presence of APC and PCAT Attenuation Grade

ROC analysis of $PCAT_{Lesion}$ showed that the cutoff value for identifying patients with PMI was −80.7 HU (sensitivity, 66.7%; specificity, 82.5%; AUC, 0.75 [95% CI, 0.62–0.88]) on 70-kVp images and −72.9 HU (sensitivity, 55.2%; specificity, 85.7%; AUC, 0.72 [95% CI, 0.59–0.85]) on 100- to 120-kVp images. Based on these cutoff values, the lesions were categorized into high PCAT ($PCAT_{Lesion} \geq−80.7$ HU on 70-kVp images or $PCAT_{Lesion} \geq−72.9$ HU on 100- to 120-kVp images) or low PCAT ($PCAT_{Lesion} <−80.7$ HU on 70-kVp images or $PCAT_{Lesion} <−72.9$ HU on 100- to 120-kVp images). When lesions were classified based on the presence of APCs and PCAT attenuation grade, the incidence of PMI was the highest in lesions with both APCs (+) and high PCAT (Figure 3A), which showed a higher risk for PMI than those with APCs (−) and low PCAT (OR, 24.7 [95% CI, 5.86–105.0]; $P<0.001$) (Figure 3B). Representative cases are described in Figure S3.

## Relationship Between PCAT Attenuation, Microcirculatory Dysfunction, and PMI

A significant correlation was found between PCAT attenuation and IMR, both pre-PCI ($r=0.324$, $P<0.001$) and post-PCI ($r=0.429$, $P<0.001$), and there was a weak correlation between PCAT attenuation and Δ IMR ($r=0.19$, $P=0.03$). Pre- and post-PCI IMR and Δ IMR were significantly higher in the lesions with high PCAT attenuation than in those with low PCAT attenuation (Figure 4). Moreover, a significant correlation was observed between post-PCI cTnI levels and PCAT attenuation ($r=0.29$, $P<0.001$). There were also significant correlations between post-PCI cTnI levels and post-PCI IMR ($r=0.43$, $P<0.001$) or Δ IMR ($r=0.30$, $P<0.001$) (Figure 5).

## DISCUSSION

To our knowledge, this is the first study investigating the relationship between PCAT attenuation measured using pre-PCI cCTA imaging and the occurrence of PMI among patients with CCS. This study's main findings can be summarized as follows: (1) Patients who experienced PMI after PCI had a higher level of vascular inflammation as indicated by increased PCAT attenuation at the culprit lesion, culprit vessel, and patient level. (2) In addition to older age and cCTA-derived APC, increased pre-PCI PCAT attenuation measured using cCTA and microcirculatory resistance assessed

**Figure 4.  Correlations between IMR-related variables and PCAT attenuation, and comparison of IMR-related variables according to PCAT attenuation grade.**
**A**, Pre-PCI IMR. A significant correlation was found between PCAT attenuation and pre-PCI IMR ($r=0.324$, $P<0.001$). Pre-PCI IMR in the lesions with high PCAT was significantly higher than in those with low PCAT (34.9 mm Hg×s/cm vs 26.2 mm Hg×s/cm, $P<0.001$). **B**, Post-PCI IMR. A significant correlation was found between PCAT attenuation and post-PCI IMR ($r=0.429$, $P<0.001$). Post-PCI IMR in the lesions with high PCAT was significantly higher than in those with low PCAT (42.4 mm Hg×s/cm vs 27.2 mm Hg×s/cm, $P<0.001$). **C**, Δ IMR. There was a weak correlation between PCAT attenuation and Δ IMR ($r=0.19$, $P=0.03$). Δ IMR in the lesions with high PCAT was significantly higher than in those with low PCAT (6.8 mm Hg×s/cm vs 1.0 mm Hg×s/cm, $P<0.001$). IMR indicates index of microvascular resistance; PCAT, pericoronary adipose tissue; and PCI, percutaneous coronary intervention.

**A** IMR at pre PCI

**B** IMR at post PCI

**C** Delta IMR
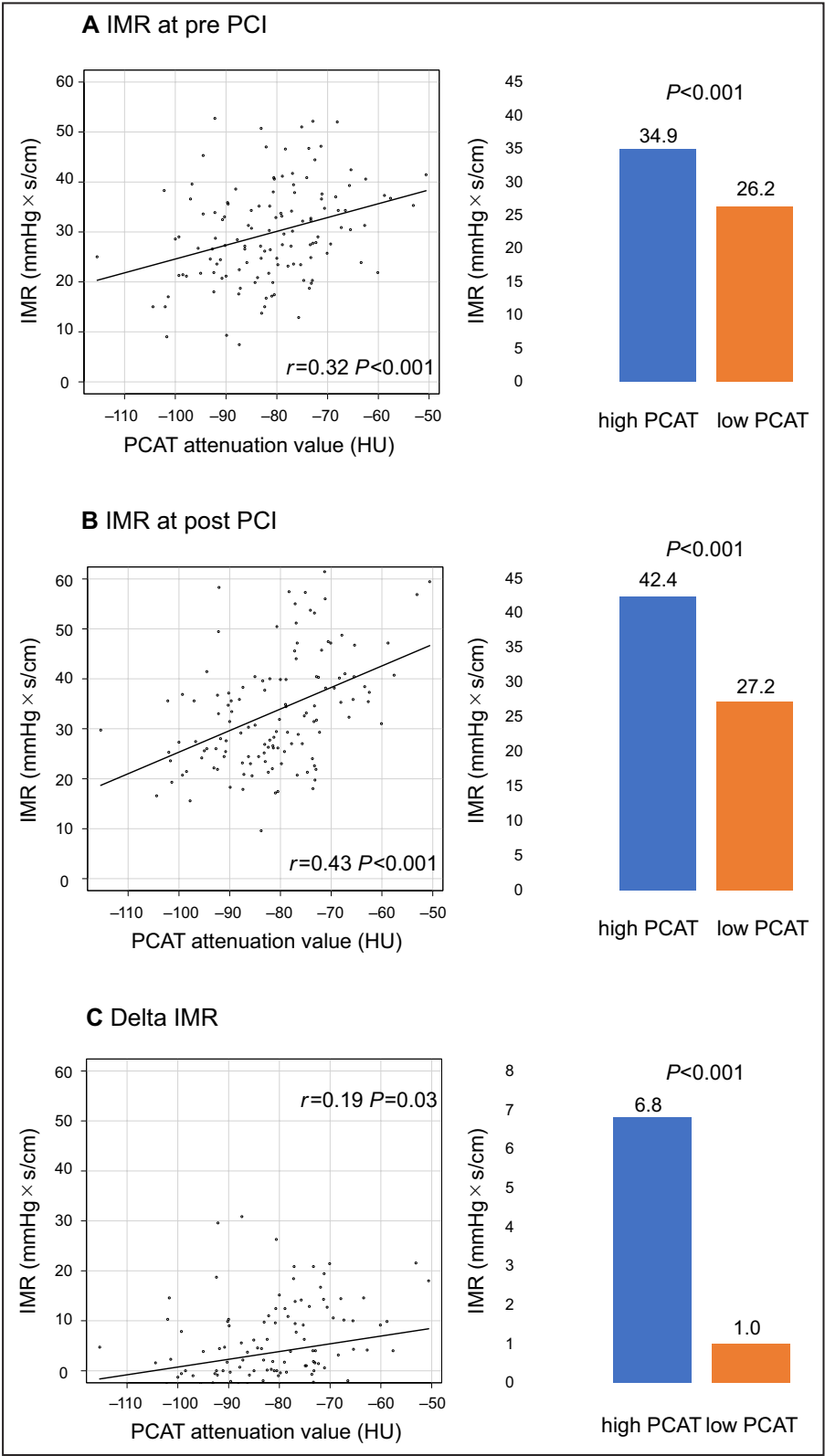
using angio-derived IMR were independently associated with the occurrence of PMI. (3) PCAT attenuation at the culprit lesion level demonstrated superior predictive ability in identifying PMI compared with PCAT attenuation at the culprit vessel and patient level. (4) PCAT attenuation at the culprit lesion level provided incremental predictive value over the model incorporating clinical risk factors and traditional cCTA findings,

including APCs, for identifying patients at risk of PMI. (5) Microcirculatory resistance significantly increased after PCI in patients with PMI but not in those without PMI. Moreover, high PCAT attenuation was significantly associated with microcirculatory dysfunction before and after PCI and its exacerbation during PCI. These findings highlight the importance of PCAT attenuation as a potential marker of vascular inflammation and its association with PMI risk. In addition, the study underscores the role of microcirculatory dysfunction in developing PMI, particularly in the context of lesions characterized by high PCAT attenuation.

## Incremental Value of Inflammation to APC

Distal coronary embolization of intracoronary thrombus and atheromatous material has been recognized as a major cause of PMI.[1] APCs observed on cCTA, such as positive remodeling, low attenuation plaque, spotty calcification, and napkin-ring sign, indicate plaque vulnerability with higher lipid content.[21,22] Consequently, plaques with APCs may be susceptible to fragmentation into numerous atherosclerotic particles after stent expansion, resulting in PMI. A prior cCTA study demonstrated a significant association between APCs on cCTA and post-PCI cTnT elevation.[5] However, a previous serial cCTA study[2] showed that many plaques with APCs remained stable and event-free >1 year, whereas some developed instability, ultimately resulting in acute coronary syndrome. This finding suggests that the presence of APCs alone may not necessarily predict the likelihood of plaque instability or its activity.[23] The present study indicated low positive predictive values for the presence of APCs alone in predicting PMI (sensitivity: 72.0%, specificity: 49.3%, positive predictive value: 48.6%, negative predictive value: 72.5%). Therefore, we currently consider that assessing APCs

alone using cCTA may be insufficient; other factors should be evaluated with cCTA to better predict PMI.

Inflammation plays a vital role in collagen degradation in the fibrous cap, which precedes fibrous cap rupture, by releasing collagen-degrading enzymes. In addition, inflammation significantly contributes to plaque thrombogenicity by providing a source of tissue factor.[24] Therefore, it is conceivable that inflammation increases plaque instability and thrombogenicity, predisposing to intraprocedural microembolization with subsequent microvascular injury or obstruction after PCI.[25] Recently, cCTA has emerged as a noninvasive method to evaluate PCAT attenuation, potentially representing adjacent vessels' inflammatory status. In a landmark study, Antonopoulos et al demonstrated a relationship between coronary perivascular fat attenuation and inflammation in and around the coronary artery.[10] In the present study, we evaluated PCAT attenuation as a measure of local coronary inflammation to obtain a more accurate risk stratification of PMI.

Consequently, we found that increased PCAT attenuation was independently associated with the occurrence of PMI. Previous studies have clarified the additive value of PCAT attenuation over APC features. Kwiecinski et al showed a correlation between PCAT attenuation and 18F-sodium fluoride (18F-NaF) activity, which provided information on plaque activity.[19] In this study, not all plaques with APCs on cCTA manifested plaque activity as assessed by 18F-NaF uptake or altered PCAT attenuation, suggesting that the presence of APCs alone may not necessarily represent plaque activity. Moreover, Oikonomou et al[26] demonstrated that APC features with low inflammation assessed by PCAT attenuation were not associated with increased cardiac risk. However, when inflammation is present, APC features can identify a particularly high-risk group of patients. Considering these findings, assessment
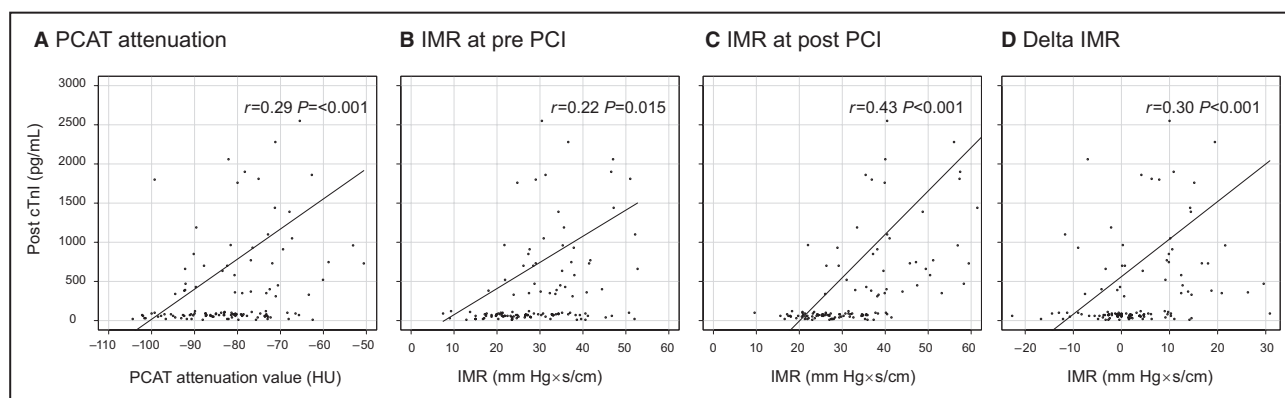


**Figure 5.  Correlations between post-PCI cTnI level and PCAT attenuation or IMR-related variables.**
**A**, PCAT attenuation. A significant correlation was found between PCAT attenuation and post-PCI cTnI ($r=0.29$, $P<0.001$). **B**, Pre-PCI IMR. A weak correlation was found between pre-PCI IMR and post-PCI cTnI ($r=0.22$, $P=0.015$). **C**, Post-PCI IMR. A significant correlation was found between post-PCI IMR and post-PCI cTnI ($r=0.43$, $P<0.001$). **D**, Δ IMR. A significant correlation was found between Δ IMR and post-PCI cTnI ($r=0.30$, $P<0.001$). cTnT indicates cardiac troponin I; IMR, index of microvascular resistance; PCAT, pericoronary adipose tissue; and PCI, percutaneous coronary intervention.

of APCs alone may be insufficient for plaque risk assessment; evaluating plaque activity by measuring increased PCAT attenuation could be important. Therefore, we speculate that inflammation assessed by PCAT attenuation could provide incremental value to the evaluation of APC, providing a more accurate risk stratification of subsequent PMI after PCI. Our study demonstrated that PCAT attenuation at the culprit lesion level provided incremental predictive value over models incorporating clinical risk factors and traditional cCTA findings, including APCs, in identifying patients at risk of PMI. Furthermore, lesions with both the presence of APCs and high PCAT attenuation had a 24.7-fold higher risk of PMI than other lesions. These findings suggest that assessing inflammation through PCAT attenuation on cCTA may help detect lesions susceptible to PMI, offering advantages over a simple evaluation based solely on APCs.

## Relationship Between Vascular Inflammation, Microcirculatory Dysfunction, and PMI

Coronary microcirculatory dysfunction represents another mechanism contributing to the occurrence of PMI. A previous study demonstrated a significant association between baseline and post-PCI IMR values and PMI. Periprocedural IMR changes were significantly higher in patients who developed PMI, with post-PCI IMR emerging as a stronger and independent predictor of PMI occurrence.[27] Consistent with these findings, the present study also revealed a significant association between microcirculatory dysfunction, as assessed using angio-based pre- and post-PCI IMR, and periprocedural IMR changes with PMI. Moreover, our study clarified the relationship between local inflammatory status, microcirculatory dysfunction, and the occurrence of PMI. Lesions with high PCAT attenuation had significantly higher pre- and post-PCI IMR and Δ IMR than those with low PCAT attenuation. In addition, there were weak but statistically significant correlations between PCAT attenuation and IMR-related variables. Furthermore, this study showed that both pre-PCI PCAT levels and microcirculatory deterioration during PCI significantly correlated with post-PCI cTnI levels, representing the extent of myocardial necrosis due to PCI. These findings suggest a substantial association between local vessel inflammation, preexisting microcirculatory dysfunction, and likelihood of exacerbating microcirculatory dysfunction due to PCI, ultimately contributing to PMI occurrence. The detailed mechanisms remain speculative; however, we believe that local vessel inflammation may indicate increased plaque vulnerability and instability, accelerating atheromatous embolization, thrombogenicity, and microcirculatory dysfunction. Notably, even after excluding cases with transient or final no-reflow phenomenon, post-PCI IMR values remained higher in the PMI group when compared with those in the non-PMI group. These findings emphasize that, even in cases where there is no angiographically apparent deterioration of coronary flow, PMI can still occur due to microcirculatory dysfunction. This reinforces our hypothesis that microcirculatory dysfunction plays a significant role in the development of PMI, particularly in the context of lesions characterized by high PCAT attenuation.

It is well established that highly vulnerable plaques contain many macrophages that secrete several inflammatory cytokines and substantial amounts of tissue factor.[28] A previous experimental study has demonstrated that the release of active tissue factors alone can lead to the occurrence of the no-reflow phenomenon.[29] Based on these findings, we speculate that during PCI, the mechanical disruption of highly inflammatory lipid-rich plaques, particularly those with APCs, may release such active tissue factors into the coronary circulation. Consequently, these circulating active tissue factors and cytokines have the potential to induce microcirculatory spasm and/or dysfunction, contributing to PMI occurrence. Moreover, baseline microcirculatory dysfunction resulting from inflammation may predispose individuals to a reduced tolerance toward further microcirculatory dysfunction induced by the mechanical damage of the epicardial coronary artery by PCI.

In addition, inflamed plaques may be prone to embolization of plaque debris and thrombotic aggregates, further exacerbating microcirculatory dysfunction. The combined effects of inflammation on plaque instability and microcirculatory dysfunction play a significant role in PMI occurrence. Therefore, assessing inflammation through PCAT attenuation on cCTA may provide additive information on the activity of plaques with APCs and microcirculatory dysfunction in the coronary vessel. Further studies are necessary to confirm our findings.

## Different Predictive Abilities in Identifying PMI Among Lesion-, Vessel-, and Patient-Level PCAT Attenuation

In the present study, PCAT attenuation at the culprit lesion level demonstrated superior predictive ability in identifying PMI compared with PCAT attenuation at the culprit vessel and patient level. This suggests that lesion-specific local inflammation may have a greater impact on PMI occurrence than inflammation at the vessel or patient level. The level at which PCAT attenuation should be measured to assess inflammation remains controversial. Recently, several studies have investigated relationships between lesion-specific PCAT attenuation and culprit lesion

plaque vulnerability. Goeller et al[17] showed that PCAT attenuation was higher around culprit lesions than nonculprit lesions in patients with acute coronary syndromes or in control subjects with stable coronary artery disease. In addition, the authors reported that low attenuation plaque was independently associated with high PCAT attenuation at the culprit lesion level. These findings highlighted the potential importance of a lesion-specific evaluation of PCAT attenuation to assess local plaque characteristics. Furthermore, by evaluating plaques in all coronary segments, Kwiecinski et al[19] found that those with 18F-NaF uptake had higher PCAT attenuation than those without increased tracer activity. This relationship was not observed when only the proximal RCA was assessed for PCAT. These findings suggest that a lesion-specific assessment of PCAT may provide greater insight into atherosclerosis activity than RCA measurements or evaluation of the proximal segments of the major arteries alone. Considering that vulnerability and instability in local plaques contribute to PMI occurrence, it appears appropriate to evaluate PCAT attenuation at the culprit lesion level for predicting the occurrence of PMI, as shown in the present study.

## Limitations

First, we acknowledge that the small sample size of the present study may increase the potential for selection bias. Additionally, our study focused on a specific, high-risk patient population with a retrospective design that required recent prior CT scans. Furthermore, the observed rate of PMI in our research may appear relatively high. It is also important to emphasize that in this single-center study, there remains a possibility of bias due to unmeasured confounding. Although we have made diligent efforts to account for known confounders and have used rigorous statistical methods, the possibility of unmeasured confounding cannot be completely eliminated in any observational study. Moreover, the observational nature of the data limits the ability to draw definitive conclusions. Therefore, caution is advised when generalizing the clinical implications of our findings. It is also important to highlight that our results should undergo confirmation through external validation. A large-scale prospective study is warranted to validate the usefulness of PCAT attenuation in treatment decision making. Second, we did not directly measure coronary inflammation; however, recent studies have shown an association between PCAT attenuation and biopsy-proven vascular inflammation in patients undergoing cardiac surgery.[10] This supports the potential of PCAT attenuation as a surrogate marker for coronary inflammation. Third, it should be noted that various CT tube voltages influenced PCAT attenuation. However, even when applying different optimal cutoff values of PCAT$_{Lesion}$ according to tube voltage, the incidence of PMI was high in lesions with high PCAT attenuation, regardless of the tube voltage used (70- or 100- to 120-kVp) (Figure 4A). Fourth, we excluded severely calcified lesions in the present study. There is a lack of data on lesion-specific PCAT attenuation in the presence of severe calcification at the exact lesion site. In addition, the spatial resolution of CT may limit PCAT assessment in areas adjacent to heavy coronary calcification, affecting the evaluation of luminal stenosis and APCs. Furthermore, using rotational atherectomy in 9 of 16 severely calcified lesions during the index PCI could introduce debris and potentially influence microcirculatory dysfunction, necessitating differentiation between PMI caused by rotational atherectomy and PMI from other factors. Fifth, the PCAT attenuation at the culprit lesion level was the best predictor in this retrospective study. However, the limitations of measuring lesion-specific PCAT attenuation when the exact lesion or location undergoing PCI is uncertain. Therefore, as a noninvasive risk marker, PCAT at the vessel or RCA level might be a more feasible risk marker evaluated before PCI. Sixth, in regard to the selection of confounding variables, we acknowledge that it is a complex process with inherent limitations. In our study, we carefully considered variables such as age, hypertension, diabetes, smoking, plaque measurements such as lesion length, and other pertinent factors consistently associated with PMI in prior studies.[30,31] In addition, when constructing the multivariable model, we aimed to include clinically significant variables and potential confounders based on established literature and expert consensus. Despite accounting for these clinically relevant variables, we found that PCAT attenuation demonstrated incremental predictive value for PMI beyond their influence. Conversely, it is worth noting that our models included 11 predictors, which may seem extensive, particularly given the relatively small sample size and the number of events. Therefore, we also presented the results of the multivariable logistic regression analysis with a reduced set of covariates. Even when restricting the predictive model to the most critical variables, PCAT continued to demonstrate incremental predictive value (as shown in Data S1). Seventh, given the relatively small sample size and constraints on internal cross-validation, there is a possibility of overfitting in the AUC results. Finally, IMR-related variables were measured using an angio-based rather than a wire-based approach. Wire-based IMR evaluation is the current gold standard; a previous validation study has demonstrated that IMR derived solely from a single angiographic view can be a feasible computational alternative to pressure wire-based IMR, with good diagnostic accuracy in assessing microcirculatory dysfunction.[14]

# CONCLUSIONS

The noninvasively determined PCAT attenuation at the culprit lesion level in patients with CCS was independently associated with PMI occurrence. Adding PCAT attenuation at the culprit lesion level to cCTA-derived APCs may provide incremental benefit for identifying PMI. Our results highlight the importance of microcirculatory dysfunction in PMI development, particularly in the presence of lesions characterized by high PCAT attenuation.

## ARTICLE INFORMATION

### Affiliation

Division of Cardiovascular Medicine, Department of Internal Medicine, Kobe University Graduate School of Medicine, Kobe, Japan.

### Sources of Funding

### Disclosures

None.

### Supplemental Material

Data S1
Table S1
Figures S1–S3

## REFERENCES

1. Bulluck H, Paradies V, Barbato E, Baumbach A, Bøtker HE, Capodanno D, De Caterina R, Cavallini C, Davidson SM, Feldman DN, et al. Prognostically relevant periprocedural myocardial injury and infarction associated with percutaneous coronary interventions: a consensus document of the ESC Working Group on Cellular Biology of the Heart and European Association of Percutaneous Cardiovascular Interventions (EAPCI). *Eur Heart J*. 2021;42:2630–2642. doi: 10.1093/eurheartj/ehab271

2. Motoyama S, Ito H, Sarai M, Kondo T, Kawai H, Nagahara Y, Harigaya H, Kan S, Anno H, Takahashi H, et al. Plaque characterization by coronary computed tomography angiography and the likelihood of acute coronary events in mid-term follow-up. *J Am Coll Cardiol*. 2015;66:337–346. doi: 10.1016/j.jacc.2015.05.069

3. Patel VG, Brayton KM, Mintz GS, Maehara A, Banerjee S, Brilakis ES. Intracoronary and noninvasive imaging for prediction of distal embolization and periprocedural myocardial infarction during native coronary artery percutaneous intervention. *Circ Cardiovasc Imaging*. 2013;6:1102–1114. doi: 10.1161/CIRCIMAGING.113.000448

4. Sato A, Aonuma K. Coronary plaque morphology on multi-modality imagining and periprocedural myocardial infarction after percutaneous coronary intervention. *Int J Cardiol Heart Vasc*. 2016;11:43–48. doi: 10.1016/j.ijcha.2016.03.009

5. Watabe H, Sato A, Akiyama D, Kakefuda Y, Adachi T, Ojima E, Hoshi T, Murakoshi N, Ishizu T, Seo Y, et al. Impact of coronary plaque composition on cardiac troponin elevation after percutaneous coronary intervention in stable angina pectoris: a computed tomography analysis. *J Am Coll Cardiol*. 2012;59:1881–1888. doi: 10.1016/j.jacc.2012.01.051

6. Ross R. Atherosclerosis—an inflammatory disease. *N Engl J Med*. 1999;340:115–126. doi: 10.1056/NEJM199901143400207

7. Tanaka A, Imanishi T, Kitabata H, Kubo T, Takarada S, Tanimoto T, Kuroi A, Tsujioka H, Ikejima H, Komukai K, et al. Lipid-rich plaque and myocardial perfusion after successful stenting in patients with non-ST-segment elevation acute coronary syndrome: an optical coherence tomography study. *Eur Heart J*. 2009;30:1348–1355. doi: 10.1093/eurheartj/ehp122

8. Recio-Mayoral A, Rimoldi OE, Camici PG, Kaski JC. Inflammation and microvascular dysfunction in cardiac syndrome X patients without conventional risk factors for coronary artery disease. *JACC Cardiovasc Imaging*. 2013;6:660–667. doi: 10.1016/j.jcmg.2012.12.011

9. Oikonomou EK, Marwan M, Desai MY, Mancio J, Alashi A, Hutt Centeno E, Thomas S, Herdman L, Kotanidis CP, Thomas KE, et al. Non-invasive detection of coronary inflammation using computed tomography and prediction of residual cardiovascular risk (the CRISP CT study): a post-hoc analysis of prospective outcome data. *Lancet*. 2018;392:929–939. doi: 10.1016/S0140-6736(18)31114-0

10. Antonopoulos AS, Sanna F, Sabharwal N, Thomas S, Oikonomou EK, Herdman L, Margaritis M, Shirodaria C, Kampoli AM, Akoumianakis I, et al. Detecting human coronary inflammation by imaging perivascular fat. *Sci Transl Med*. 2017;9:eaal2658. doi: 10.1126/scitranslmed.aal2658

11. Tu S, Ding D, Chang Y, Li C, Wijns W, Xu B. Diagnostic accuracy of quantitative flow ratio for assessment of coronary stenosis significance from a single angiographic view: a novel method based on bifurcation fractal law. *Catheter Cardiovasc Interv*. 2021;97(Suppl 2):1040–1047. doi: 10.1002/ccd.29592

12. Zhang Y, Zhang S, Westra J, Ding D, Zhao Q, Yang J, Sun Z, Huang J, Pu J, Xu B, et al. Automatic coronary blood flow computation: validation in quantitative flow ratio from coronary angiography. *Int J Cardiovasc Imaging*. 2019;35:587–595. doi: 10.1007/s10554-018-1506-y

13. Tu S, Echavarria-Pinto M, von Birgelen C, Holm NR, Pyxaras SA, Kumsars I, Lam MK, Valkenburg I, Toth GG, Li Y, et al. Fractional flow reserve and coronary bifurcation anatomy: a novel quantitative model to assess and report the stenosis severity of bifurcation lesions. *JACC Cardiovasc Interv*. 2015;8:564–574. doi: 10.1016/j.jcin.2014.12.232

14. Fan Y, Fezzi S, Sun P, Ding N, Li X, Hu X, Wang S, Wijns W, Lu Z, Tu S. In vivo validation of a novel computational approach to assess microcirculatory resistance based on a single angiographic view. *J Pers Med*. 2022;12:1798. doi: 10.3390/jpm12111798

15. Tu S, Westra J, Yang J, von Birgelen C, Ferrara A, Pellicano M, Nef H, Tebaldi M, Murasato Y, Lansky A, et al. Diagnostic accuracy of fast computational approaches to derive fractional flow reserve from diagnostic coronary angiography: the international multicenter FAVOR pilot study. *JACC Cardiovasc Interv*. 2016;9:2024–2035. doi: 10.1016/j.jcin.2016.07.013

16. Abbara S, Blanke P, Maroules CD, Cheezum M, Choi AD, Han BK, Marwan M, Naoum C, Norgaard BL, Rubinshtein R, et al. SCCT guidelines for the performance and acquisition of coronary computed tomographic angiography: a report of the Society of Cardiovascular Computed Tomography Guidelines Committee: endorsed by the north American Society for Cardiovascular Imaging (NASCI). *J Cardiovasc Comput Tomogr*. 2016;10:435–449. doi: 10.1016/j.jcct.2016.10.002

17. Goeller M, Achenbach S, Cadet S, Kwan AC, Commandeur F, Slomka PJ, Gransar H, Albrecht MH, Tamarappoo BK, Berman DS, et al. Pericoronary adipose tissue computed tomography attenuation and high-risk plaque characteristics in acute coronary syndrome compared with stable coronary artery disease. *JAMA Cardiol*. 2018;3:858–863. doi: 10.1001/jamacardio.2018.1997

18. Maurovich-Horvat P, Ferencik M, Voros S, Merkely B, Hoffmann U. Comprehensive plaque assessment by coronary CT angiography. *Nat Rev Cardiol*. 2014;11:390–402. doi: 10.1038/nrcardio.2014.60

19. Kwiecinski J, Dey D, Cadet S, Lee SE, Otaki Y, Huynh PT, Doris MK, Eisenberg E, Yun M, Jansen MA, et al. Peri-coronary adipose tissue density is associated with $^{18}$F-sodium fluoride coronary uptake in stable patients with high-risk plaques. *JACC Cardiovasc Imaging*. 2019;12:2000–2010. doi: 10.1016/j.jcmg.2018.11.032

20. Yuvaraj J, Lin A, Nerlekar N, Munnur RK, Cameron JD, Dey D, Nicholls SJ, Wong DTL. Pericoronary adipose tissue attenuation is associated with high-risk plaque and subsequent acute coronary syndrome in patients with stable coronary artery disease. *Cells*. 2021;10:1143. doi: 10.3390/cells10051143

21. Schoenhagen P, Ziada KM, Kapadia SR, Crowe TD, Nissen SE, Tuzcu EM. Extent and direction of arterial remodeling in stable versus unstable coronary syndromes: an intravascular ultrasound study. *Circulation*. 2000;101:598–603. doi: 10.1161/01.CIR.101.6.598

22. Nakazato R, Otake H, Konishi A, Iwasaki M, Koo BK, Fukuya H, Shinke T, Hirata K, Leipsic J, Berman DS, et al. Atherosclerotic plaque characterization by CT angiography for identification of high-risk coronary artery lesions: a comparison to optical coherence tomography. *Eur Heart J Cardiovasc Imaging*. 2015;16:373–379. doi: 10.1093/ehjci/jeu188

23. Narula J, Kovacic JC. Putting TCFA in clinical perspective. *J Am Coll Cardiol*. 2014;64:681–683. doi: 10.1016/j.jacc.2014.06.1163

24. Shah PK. Inflammation and plaque vulnerability. *Cardiovasc Drugs Ther*. 2009;23:31–40. doi: 10.1007/s10557-008-6147-2

25. Tucker B, Vaidya K, Cochran BJ, Patel S. Inflammation during percutaneous coronary intervention-prognostic value, mechanisms and therapeutic targets. *Cells*. 2021;10:1391. doi: 10.3390/cells10061391

26. Oikonomou EK, Desai MY, Marwan M, Kotanidis CP, Antonopoulos AS, Schottlander D, Channon KM, Neubauer S, Achenbach S, Antoniades C. Perivascular fat attenuation index stratifies cardiac risk associated with high-risk plaques in the CRISP-CT study. *J Am Coll Cardiol*. 2020;76:755–757. doi: 10.1016/j.jacc.2020.05.078

27. Mangiacapra F, Bressi E, Di Gioia G, Pellicano M, Di Serafino L, Peace AJ, Bartunek J, Morisco C, Wijns W, De Bruyne B, et al. Coronary microcirculation and peri-procedural myocardial injury during elective percutaneous coronary intervention. *Int J Cardiol*. 2020;306:42–46. doi: 10.1016/j.ijcard.2019.12.042

28. Sakakura K, Nakano M, Otsuka F, Ladich E, Kolodgie FD, Virmani R. Pathophysiology of atherosclerosis plaque progression. *Heart Lung Circ*. 2013;22:399–411. doi: 10.1016/j.hlc.2013.03.001

29. Bonderman D, Teml A, Jakowitsch J, Adlbrecht C, Gyöngyösi M, Sperker W, Lass H, Mosgoeller W, Glogar DH, Probst P, et al. Coronary no-reflow is caused by shedding of active tissue factor from dissected atherosclerotic plaque. *Blood*. 2002;99:2794–2800. doi: 10.1182/blood.V99.8.2794

30. Park DW, Kim YH, Yun SC, Ahn JM, Lee JY, Kim WJ, Kang SJ, Lee SW, Lee CW, Park SW, et al. Frequency, causes, predictors, and clinical significance of peri-procedural myocardial infarction following percutaneous coronary intervention. *Eur Heart J*. 2013;34:1662–1669. doi: 10.1093/eurheartj/eht048

31. Uetani T, Amano T, Kunimura A, Kumagai S, Ando H, Yokoi K, Yoshida T, Kato B, Kato M, Marui N, et al. The association between plaque characterization by CT angiography and post-procedural myocardial infarction in patients with elective stent implantation. *JACC Cardiovasc Imaging*. 2010;3:19–28. doi: 10.1016/j.jcmg.2009.09.016